THE JOURNAL OF BIOLOGICAL CHEMISTRY VOL. 281, NO. 43, pp. 32774–32783, October 27, 2006

Siglec-7 Undergoes a Major Conformational Change When Complexed with the α(2,8)-Disialylganglioside GT1b*

Received for publication, February 22, 2006 Published, JBC Papers in Press, August 8, 2006, DOI 10.1074/jbc.M601714200

Helen Attrill[‡§], **Akihiro Imamura**[¶], **Ritu S. Sharma**[§], **Makoto Kiso**[¶], **Paul R. Crocker**[§1], **and Daan M. F. van Aalten**[‡1,2]

From the [‡]*Divisions of Biological Chemistry and Molecular Microbiology and* [§]*Cell Biology and Immunology, School of Life Sciences, University of Dundee, Dundee DD1 5EH, Scotland, United Kingdom and* [¶]*Department of Applied Bioorganic Chemistry, Faculty of Applied Biological Sciences, Gifu University, 1-1 Yanagido, Gifu-shi, Gifu 501-1193, Japan*

The siglecs are a group of mammalian sialic acid binding receptors expressed predominantly in the immune system. The CD33-related siglecs show complex recognition patterns for sialylated glycans. Siglec-7 shows a preference for α(2,8)-disialylated ligands and provides a structural template for studying the key interactions that drive this selectivity. We have co-crystallized Siglec-7 with a synthetic oligosaccharide corresponding to the α(2,8)-disialylated ganglioside GT1b. The crystal structure of the complex offers a first glimpse into how this important family of lectins binds the structurally diverse gangliosides. The structure reveals that the C-C′ loop, a region implicated in previous studies as driving siglec specificity, undergoes a dramatic conformational shift, allowing it to interact with the underlying neutral glycan core of the ganglioside. The structural data in combination with mutagenesis studies show that binding of the ganglioside is driven by extensive hydrophobic contacts together with key polar interactions and that the binding site structure is complementary to preferred solution conformations of GT1b.

Siglecs are a group of evolutionary conserved receptors that constitute the major subgroup of the I-type lectin family (1–3). Siglecs recognize sialic acid, a nine-carbon sugar that often caps the non-reducing end of glycans (4). Engagement of specific sialylated ligands by siglecs is thought to influence cellular adhesion, recognition, and signaling in the immune and nervous systems (5–8).

With the exceptions of myelin-associated glycoprotein (MAG, Siglec-4), found in the nervous system (9, 10), and Siglec-6, expressed on placental trophoblast cells (11), siglec expression appears to be restricted to cells of the hemopoietic and immune systems. Eleven siglecs have been described in humans; of these, eight belong to the recently characterized CD33-related siglec sub-family (CD33/Siglec-3 and Siglec-5–11) (12). This subfamily and the B cell inhibitory receptor, CD22/Siglec-2, can suppress immune cell activation by the recruitment of the SH2 domain containing phosphatases SHP-2 and/or SHP-1 to their cytoplasmic domain tyrosine-based motifs (13, 14).

The siglec sialic acid binding site resides in the membrane distal N-terminal domain, marked by a conserved arginine that forms a crucial salt bridge with the sialic acid carboxylate. Although the primary binding determinant is the sialic acid, the underlying glycan core is key to individual siglec binding specificity (5). The ligand binding preference for most siglecs has been characterized using the common capping structures found on *N*- and *O*-glycans (15) and glycan arrays, but the *in vivo* targets are less well defined. One potential target for siglec binding are gangliosides; that is, glycolipids, which consist of a ceramide linked to a sialylated glycan. All share a common lacto-ceramide core (Galβ(1,4)Glcβ(1-1′)Cer). Diversity is generated by the addition of other neutral sugars and sialic acid in different linkages (and modification of sialic acid itself) (16).

Siglec-7 is an inhibitory receptor expressed on NK cells and to a lesser extent, monocytes and a subset of CD8+ T cells (13, 17–21). *In vitro* binding studies have revealed that Siglec-7 shows a marked preference for glycoconjugates bearing α(2,8)-linked disialic acid and branched α(2,6)-linked sialic acid (22). The α(2,8)-linked disialic acid moiety is present in b-series gangliosides (and other gangliosides such as GT1a and GD1c). Importantly, Nicoll *et al.* (21), have demonstrated that a b-series ganglioside, GD3,[3] when expressed on target cells, was able to mediate interactions with Siglec-7 expressed on NK cells, leading to the suppression of NK mediated cytolytic activity. This disialyl motif has also been identified on the serum glycoproteins fetuin, α2-macrogobulin, and adipo Q (23), neural cell adhesion molecule in the central nervous system (24), and a 70-kDa glycoprotein found on T cells (25).

Previously, we have described the structure of Siglec-7 as a prototypic template for the CD33-related siglec subfamily and shown the mode of binding for the primary sialic acid (26, 27). We now present the crystal structure of Siglec-7 in complex with a GT1b ganglioside analog. This structure reveals for the

* This work was supported in part by Biotechnology and Biological Sciences Research Council, Swindon, United Kingdom Grant B14 010 (to P. R. C. and D. v. A.). The costs of publication of this article were defrayed in part by the payment of page charges. This article must therefore be hereby marked "*advertisement*" in accordance with 18 U.S.C. Section 1734 solely to indicate this fact.

The atomic coordinates and structure factors (code 2HRL) have been deposited in the Protein Data Bank, Research Collaboratory for Structural Bioinformatics, Rutgers University, New Brunswick, NJ (http://www.rcsb.org/).

[1] Supported by Wellcome Trust Senior Research Fellowships.

[2] To whom correspondence should be addressed: Division of Biological Chemistry and Molecular Microbiology, School of Life Sciences, University of Dundee, Dundee DD1 5EH, Scotland, UK. Tel.: 44-1382-344979; Fax: 44-1382-345764; E-mail: dava@davapc1.bioch.dundee.ac.uk.

[3] The abbreviations used are: GD3, Neu5Acα(2,8)Neu5Acα(2,3)Galβ(1,4)-Glcβ1-ceramide; GM3, Neu5Acα(2,3)Galβ(1,4)Glcβ1-ceramide; GM1, Galβ-(1,3)GalNAcβ(1,4)(Neu5Acα(2,3))Galβ(1,4)Glcβ1-ceramide; PDB, Protein Data Bank; dSL, Neu5Acα(2,8)Neu5Acα(2,3)Galβ(1,4)Glcβ1, disialyllactose.

first time how Siglec-7 can form intimate associations with a complex oligosaccharide ligand, leading to a dramatic conformational change in the protein.

EXPERIMENTAL PROCEDURES

Synthesis of GT1b—The GT1b analog (see Fig. 1*A*) was synthesized from the lactose derivative 2-(trimethylsilyl)ethyl 2,6-di-*O*-benzyl-β-D-galactopyranosyl-(1→4)-2,3,6-tri-*O*-benzyl-b-D-glucopyranoside using the reaction scheme described by Ishida *et al.* (28).

Overexpression and Purification of Siglec-7 V-set Domain—The overexpression of the Siglec-7 V-set domain has previously been described (26). The V-set domain was expressed as a secreted protein from a stably transfected Chinese hamster ovary Lec1 cell line (29). The media was passed over a sheep anti-Siglec-7 polyclonal antibody affinity column and eluted with 0.1 M glycine, pH 2.5. The eluate was diluted with 1 M sodium acetate, pH 5.5, to a final concentration of 50 mM, and the pH was adjusted to 5.5. Deglycosylation was performed using 0.5 units of endoglycosidase H (Roche Applied Science)/mg of protein at 37 °C for 16 h. A gel filtration step was performed using a Superdex 75 26/60 (GE Healthcare) column in 25 mM Tris, pH 8.0, 75 mM NaCl.

Crystallization and Data Collection—The protein was concentrated to 8 mg/ml and incubated with a 20-fold molar excess of the GT1b analog. Crystallization was performed using sitting drop vapor diffusion (crystallization platforms were purchased from Douglas Instruments) screening with Crystal Screens I and II (Hampton Research) at 20 °C. Crystals grew in Crystal Screen I, condition 28 (200 mM sodium acetate, 100 mM sodium cacodylate, pH 6.5, and 30% w/v polyethylene glycol 8000) and were cryoprotected with 10% glycerol before freezing under a stream of nitrogen gas. Data were collected to 1.85 Å at beamline ID14-EH4 at the European Synchrotron Radiation Facility at 100 K.

Structure Determination and Refinement—Data were processed and scaled by the HKL suite of programs (30) (see Table 1). Molecular replacement was performed using AMoRe (31) using the Siglec-7 apo structure PDB code 1O7S. One outstanding solution, with an *R*-factor of 42.4 and correlation coefficient of 50.7, was found. ARP/wARP (32) built 99 of 127 residues using the model phases from molecular replacement. Initial refinement was carried out in CNS (33), interspersed with manual manipulation in O (34), and followed by refinement using Refmac5 (35). After model refinement and inclusion of waters, the five sugar residues and the trimethylsilyl group of the GT1b analog were built into good quality $|F_o| - |F_c|$, φ_{calc} density in the binding site (see Fig. 1*B*). Ligand coordinates and topology were generated using PRODRG (36). The final model has an *R*-factor of 19.5% and an R_{free} of 23.4%, with all non-glycine residues in the most favorable and allowed regions of the Ramachandran plot (see Table 1 for statistical analysis).

Site-directed Mutagenesis and Expression of Chimeras—Mutagenesis was performed using the QuikChange site-directed mutagenesis kit (Stratagene) on a Siglec-7-Fc chimeric construct in a modified pEE14 plasmid. Successful mutagenesis was confirmed by sequencing. The plasmids were transiently transfected into COS-1 cells using FuGENE 6 transfection reagent (Roche Applied Science). The cells were cultured for a further 5 days in X-VIVO 10 serum-free media (BioWhittaker), and the supernatant was harvested. Siglec-7-Fc concentration was assayed by enzyme-linked immunosorbent assay (ELISA), and correct folding was confirmed by ELISA using anti-Siglec-7 monoclonal antibodies (7.7a and 7.5a (18)).

TABLE 1
Data collection and refinement statistics
The values within parentheses refer to the highest resolution shell.

Data collection	
Wavelength (Å)	0.9756
Resolution (Å)	15-1.85 (1.92-1.85)
Space group	$P3_221$
Unit cell (Å)	
A	46.02
B	46.02
C	106.47
Reflections	
Observed	42,394
Unique	11,626
Redundancy	3.6 (2.3)
R_{merge}	0.073 (0.52)
$I/\sigma I$	25.5 (2.3)
Completeness (%)	99.3 (98.4)
R_{free} reflections	551
R_{cryst} (%)	19.5
R_{free} (%)	23.4
Refinement	
Total number of atoms	
Protein	971
Water	54
N-Linked glycan	14
GT1b	82
⟨B⟩ Protein	24.39
⟨B⟩ Water	29.61
⟨B⟩ *N*-Linked glycan	35.01
⟨B⟩ GT1b	28.25
Root mean square deviation from ideal geometry	
Bond lengths (Å)	0.011
Bond angles (°)	1.5
Main chain B (Å²)	1.3

GT1b Ganglioside Binding Assays and Competition Assays—For the GT1b binding assay Cellstar 96-well plates (Greiner) were coated with 100 μl/well of 5 μg/ml GT1b ganglioside (Calbiochem) in methanol containing 5 μg/ml cholesterol (Sigma) and left to air dry overnight. The plates were washed 3 times in PBA (phosphate-buffered saline, 0.1% bovine serum albumin, 10 mM sodium azide) and blocked with 5% milk powder in PBA. 0.9 μg/ml Siglec-7-Fc fusion proteins were precomplexed with a 1/2000 dilution of an alkaline phosphatase anti-human IgG Fc antibody (Sigma) for 30 min at room temperature, and 50 μl/well was added to the each well. After a 2-h incubation at room temperature the plates were washed extensively; the final washes were with Tris-buffered saline, pH 7.4. 100 μl of 10 μM fluorescein diphosphate (Molecular probes) was added to each well, and fluorescence measurements were taken at intervals between 5 and 30 min using a Cytofluor (PerSeptive Biosystems) plate reader.

For competition assays, 96-well plates were coated with GT1b ganglioside at 2.5 μg/ml. Precomplexed Siglec-7-Fc (1 μg/ml) was incubated in the presence of either the GT1b analog or GD3 oligosaccharide for 15 min before the addition to GT1b-coated wells.

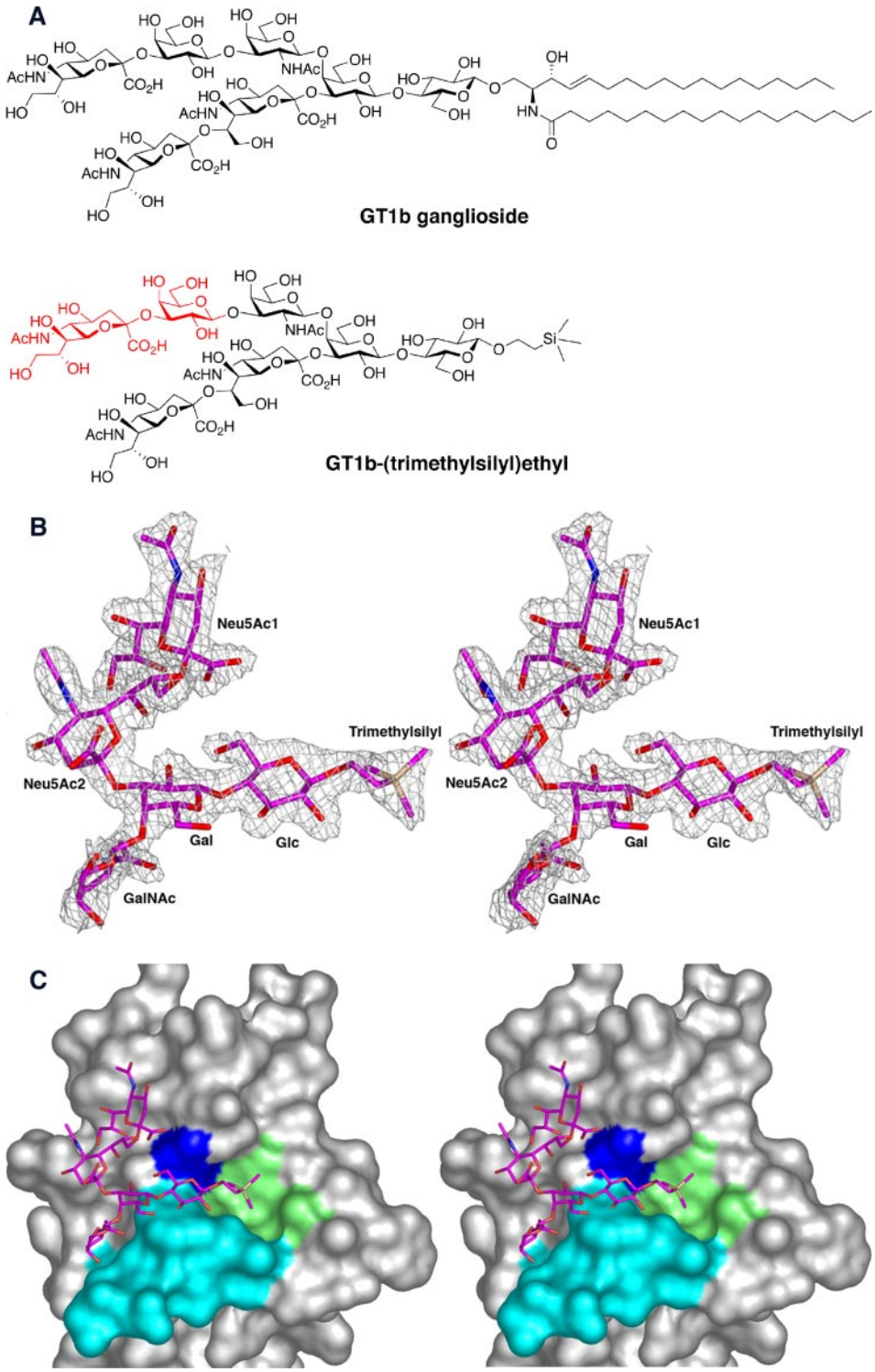

FIGURE 1. **Binding of the GT1b analog by Siglec-7.** *A*, schematic representations of GT1b ganglioside (*top*) and the GT1b analog (*bottom*) are shown. Sugars not seen in the electron density are in *red*. *B*, the V-set domain of Siglec-7 was co-crystallized with a GT1b analog. For five of the seven sugar residues there was clearly defined in the electron density. A stereo image of the unbiased $|F_o| - |F_c|$, φ_{calc} map contoured at 2.5 σ (*gray meshwork*) is shown. *C*, a stereo image of the glycan binding site surface. The ligand binding site is very open, and GT1b lies exposed to the solvent. The C-C′ loop forms a convex shelf (*marine blue*), forming the base of the binding site over which the terminal of the glycan lies. The only portion of the ligand that is buried to any significant degree is the trimethylsilyl group that lies in a hydrophobic cup (*green*). Arg-124, the essential anchor-residue, is *blue*. *D*, the network of potential hydrogen bonds (as defined by WHATIF, Table 2) are shown as *black-dashed lines*. Several water molecules are stably associated with the ligand and are shown as *orange spheres*. *E*, the human CD33-related siglecs were aligned using ClustalW (58) and annotated using aln2als (courtesy of Charlie Bond, University of Dundee). The CD33-related siglecs share between 50 and 80% sequence identity in their extracellular domains. Residues showing 100% sequence conservation are shaded in *black*; at a lower cutoff of 75% identity the shading is *gray*. The secondary structure, as defined by the liganded form of Siglec-7, is depicted by *arrows* (β-sheets) and *cylinders* (α-helices) lying *above* the *alignment*. Residues of importance are highlighted by symbols lying beneath the alignment: ⋆, essential Arg; ●, direct interaction with glycan; △, hydrophobic pocket residues which interact with the trimethylsilyl group; ▽, position equivalent to Trp-85 in Siglec-7.

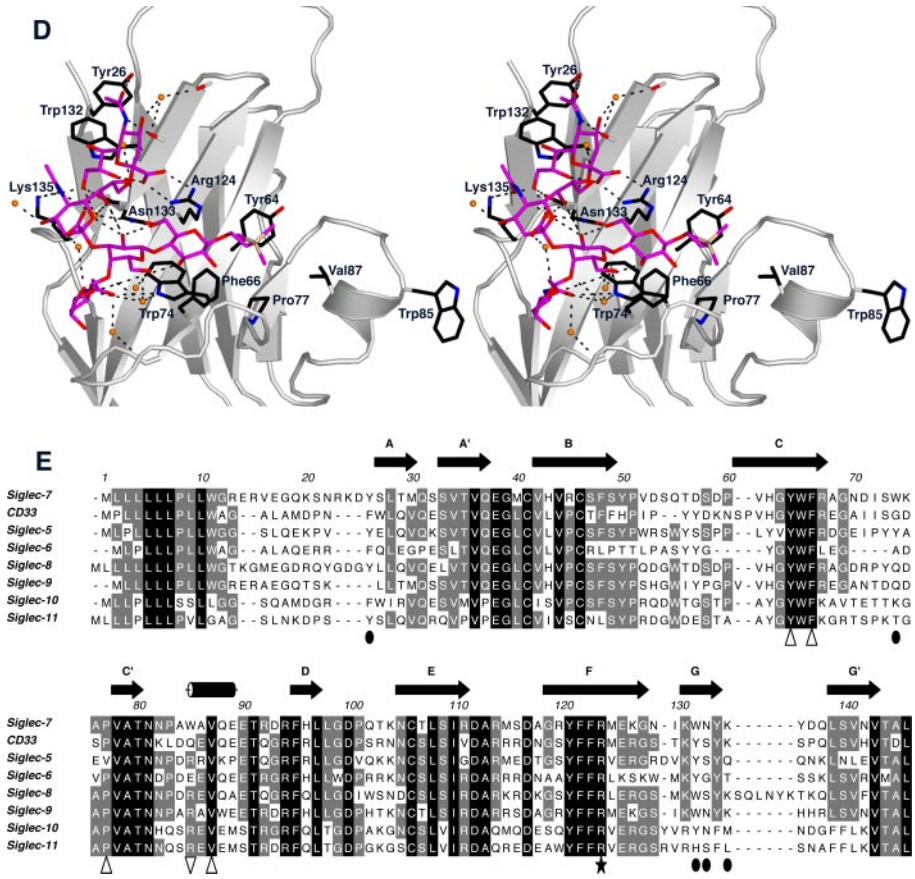

FIGURE 1–*continued*

RESULTS

Overall Structure—The Siglec-7 V-set domain was expressed as a secreted protein from *N*-acetylglucosaminyltransferase I mutant cell line, Chinese hamster ovary Lec1 (29). The resulting *N*-linked glycosylation, at Asn-105, is a homogenous high mannose structure ($GlcNAc_2Man_5$) that can be removed by endoglycosidase H digestion, leaving one GlcNAc residue. Deglycosylated Siglec-7 was co-crystallized with a GT1b analog, in which a 2-(trimethylsilyl)ethyl group replaces the ceramide portion. The complex crystallized in a hexagonal space group, as opposed to the tetragonal forms previously seen with the glycosylated, unliganded forms. Synchrotron data were collected, and the complex was solved using molecular replacement. The structure was refined to 1.85 Å, with overall good statistics (see Table 1 and "Experimental Procedures").

The structure of unliganded Siglec-7, as described previously (26), is an Ig-like fold; that is, a β-sandwich formed by two β-sheets (strands A′GFCC′ and ABED). The glycan binding site is solvent-exposed, lying on the A′GFCC′ face. Excellent quality $|F_o| - |F_c|$, φ_{calc} density was seen in the binding site for the GT1b analog, allowing 5 sugar residues and the 2-(trimethylsilyl)ethyl group to be accurately modeled (Fig. 1*B*). Five (*underlined*) of the seven sugars of the GT1b analog, Neu5Acα(2,3)Galβ (1,3)GalNAcβ(1,4)[Neu5Acα(2,8)Neu5Acα(2,3)]Galβ(1,4)Glcβ1-$(CH_2)_2Si(CH_3)_3$, are clearly defined in the electron density; the α(2,3)-linked sialic acid branch is not well defined.

Examination of the gross anatomy of the GT1b binding site (Fig. 1*C*) reveals that the site is solvent-exposed; the top edge of the binding site (as defined by the primary sialic acid) is open; the binding face slopes outward from this point and is closed off at the base by a shelf formed by the C-C′ loop (Fig. 1*C*; see also Fig. 3*D*). A slight bowl-like character is created by Tyr-136 and Lys-135, which extend from the surface of the protein on the left-hand side of the binding site and the C-C′ loop shelf. The ligand lies across the surface of the binding face, burying a total surface area of 420 Å^2 (calculated by AreaIMol, CCP4 suite), lying at its branch point extended across the C-C′ loop shelf. The only portion of the ligand significantly buried is the trimethylsilyl group, which lies in a hydrophobic pocket (Fig. 1*C*).

Interaction between GT1b and Siglec-7—The ligand occupies a large area of the binding face of Siglec-7, and each sugar moiety makes a number of contacts with the protein. The GT1b analog makes 10 direct hydrogen bonds with the protein, seven water-mediated hydrogen bonds, and a number hydrophobic interactions (Fig. 1*D*). These interactions are summarized in Table 2. The ligand is held in a "bent" conformation (Fig. 1, *B–D*); the terminal sialic acid and the glucose at reducing end of the molecule, separated by two sugar residues, are only 3.8 Å apart at their closest points (C6 of Glc and O1A of Neu5Ac). This geometry is supported by interactions with the protein and by five intramolecular hydrogen bonds (Fig. 1*D* and Table 2). The conformation of the primary sialic acid allows hydrogen bonding between the C8

TABLE 2

Hydrogen bond network within the binding site

Potential hydrogen bonds within the binding site were determined using WHAT IF (60). The WHAT IF score is a description of the predicted strength/ideality of the H-bond from on a scale of 0–1 (where 1 is the highest theoretical value); a score of 0.3 is the threshold for H bonding.

Ligand-protein H-bonding			
GT1b atom	**Protein atom**	**WHAT IF score**	**Distance**
			Å
Neu5Ac1			
O1A	Arg-124 NH2	0.81	3.0
O1B	Arg-124 NH1	0.63	2.9
N5	Lys-131 CO	0.70	2.8
O5	Tyr-26 OH	0.32	3.6
O8	Asn-133 N	0.83	2.7
O9	Lys-135 NZ	0.50	2.6
O9	Asn-133 CO	0.80	2.7
Neu5Ac2			
O5	Lys-135	0.64	2.6
Glc			
O6	Asn-133 ND2	0.77	3.0
GalNAc			
O7	Trp-74 NE1	0.45	3.5

Ligand-water-protein H-bonding						
GT1b atom	**Water molecule**	**WHAT IF score**	**Distance**	**Protein atom**	**WHAT IF score**	**Distance**
			Å			Å
O4 Neu5Ac1	46	0.54	3.1	Lys-131 CO	0.57	3.7
	46			Asn-129 CO	0.89	2.9
O9 Neu5Ac1	59	0.89	3.5	Asn-133 ND2	0.94	2.8
O5 Neu5Ac2	59	0.68	3.3			
O7 Neu5Ac2	59	0.64	2.8			
O7 GalNAc	63	0.62	2.9	Ile-72 N	0.76	3.1
O4 Gal	75	0.79	3.3	Trp-74 NE	0.53	3.0
O5 Gal	75	0.42	3.3			

Ligand intramolecular H-bonding			
GT1b atom 1	**GT1b atom 2**	**WHAT IF score**	**Distance**
			Å
O1B Neu5Ac1	O8 Neu5Ac1	0.78	2.7
O6 Neu5Ac2	O2 Gal	0.73	2.7
O7 Neu5Ac2	O2 Gal	0.34	3.1
O2D Gal	O6 Glc	0.85	2.8
O5 Gal	O3 Glc	0.68	2.8

hydroxyl and the C1 carboxyl group. Such a conformation has been accessed in molecular dynamics simulations (37, 38). Four intramolecular hydrogen bonds are possible with the branch point Gal, two with Neu5Ac2, and two with Glc.

The terminal sialic acid (Neu5Ac1) is the major determinant of ligand binding, making seven direct hydrogen bonds with the protein. A key salt bridge is formed between the sialic acid carboxylate and the guanidinium group of Arg-124; mutation of this strictly conserved Arg (Fig. 1*E*) or desialylation of the ligand abolishes binding (19, 39). All substituents on the primary sialic acid interact, directly or indirectly, with the protein (Fig. 1*D*).

The subterminal sialic acid (Neu5Ac2) is orientated with it C1 carboxylate facing away from the binding site. Neu5Ac2 makes only one direct hydrogen bond with Siglec-7 via its *N*-acetyl oxygen to Lys-135. This residue also lies within hydrogen bonding distance of the Neu5Ac1 C9-OH and may, therefore, bridge these sugars. Additional contacts are made via bridging water, between Asn-133, and the *N*-acetyl oxygen and the C7 hydroxyl of Neu5Ac2. The branch-point galactose (Gal) makes no direct hydrogen bonds with Siglec-7 but interacts with Trp-74 via a water-mediated hydrogen bond. The only portion of the Neu5Acα(2,3)-linked branch for which there is electron density is the GalNAc residue, which also interacts with Trp-74.

Glucose (Glc) interacts in two ways with Trp-74 anchoring the reducing end of the glycan; a hydrophobic stacking interaction with the Glc pyranose ring and the tryptophan indole ring and a hydrogen bond between the sugar C6 hydroxyl and head group amide of Asn-133. Trp-74 lies in the C-C′ loop, a region with exceptionally high sequence divergence (Fig. 1*E*) thought to be responsible for directing Siglec-7 ligand specificity (22).

The hydrophobic trimethylsilyl group is held in a hydrophobic pocket formed by Tyr-64, Phe-66, Pro-77, and Val-87, which is exposed by the displacement of Trp-85 (discussed below). In all CD33-related siglecs the hydrophobic residues that form the pocket are conserved. The displaced tryptophan, however, is only present in Siglec-7; in the majority of CD33-related siglecs this is an arginine (Fig. 1*E*).

Glycan Conformation—With the ability to combine different monosaccharides in various linkages and to create branched structures, the information coding potential of the glycome is enormous (40, 41). A third level of structural diversity has also been proposed at the three-dimension level, where the conformer adopted by a sugar can influence the accessibility of its substituents and, therefore, impact upon receptor recognition (42).

A search of the PDB reveals that ~50 entries contain sialylated glycoconjugate ligands; of these 24 are Neu5Acα(2,3)*X*, and 8 are Neu5Acα(2,6)*X* linkages (where *X* is any hexose). Disialic acid linkages are underrepresented, and only one entry, a complex, with tetanus toxin, contains the Neu5Acα(2,8)Neu5Ac in the nat-

ural anomeric conformation (PDB code 1YYN).[4] The ligand Neu5Acα(2,8)Neu5Acα(2,3)Galβ(1,4)Glcβ1,disialyllactose (dSL), is comparable with the glycan portion of the GD3 ganglioside, which also constitutes the disialyl branch of GT1b. Comparison of tetanus toxin-dSL and Siglec-7-GT1b analog binding may, therefore, be instructive in revealing what conformations are accessible or restricted (Fig. 2*A*).

The conformation of GT1b and dSL in these crystal complexes differ by a large degree, and no two sequential residues can be superimposed. Comparison of the two ligands suggest that two factors appear to have a major impact on the glycan structure; they are the high degree of rotational freedom in the disialyl head group and the presence or absence of a branch point.

The α(2,8)disialyl linkage consists of four bonds and, therefore, has a larger degree of rotational freedom than a typical glycosidic bond. Superimposition of the primary Neu5Ac moieties and dihedral bond analysis (Table 3) demonstrates that there is a large rotational difference about the O_2-C8′ bond (where ′ represents an atom belonging to the underlying sugar). This is supported by molecular dynamics simulations (37, 38, 43), which indicate that all three staggered conformations are accessible for ϕ. Additionally, ψ and ω angles diverge significantly between ligands, demonstrating a large freedom about the O_2-C7′ and C7′-C8′ bonds. In both, the χ angle is ~160°, in the *ap* conformation. This conformation may be favored to avoid clashes between the *N*-acetyl substituent at the C5 position of the subterminal Neu5Ac and the C7-OH (Neu5Ac2) or C1 carboxylate (Neu5Ac1).

Superposition of the subterminal sialic acid (Neu5Ac2) shows that a relative rotation about the O3-C3 bond in the Neu5Acα(2,3)Gal linkage offsets the galactose rings by 90°, which may result from the

[4] Jayaraman, S., Eswaramoorthy, S., Kumaran, D., and Swaminathan, S. (2005) *Proteins* **61,** 288–295.

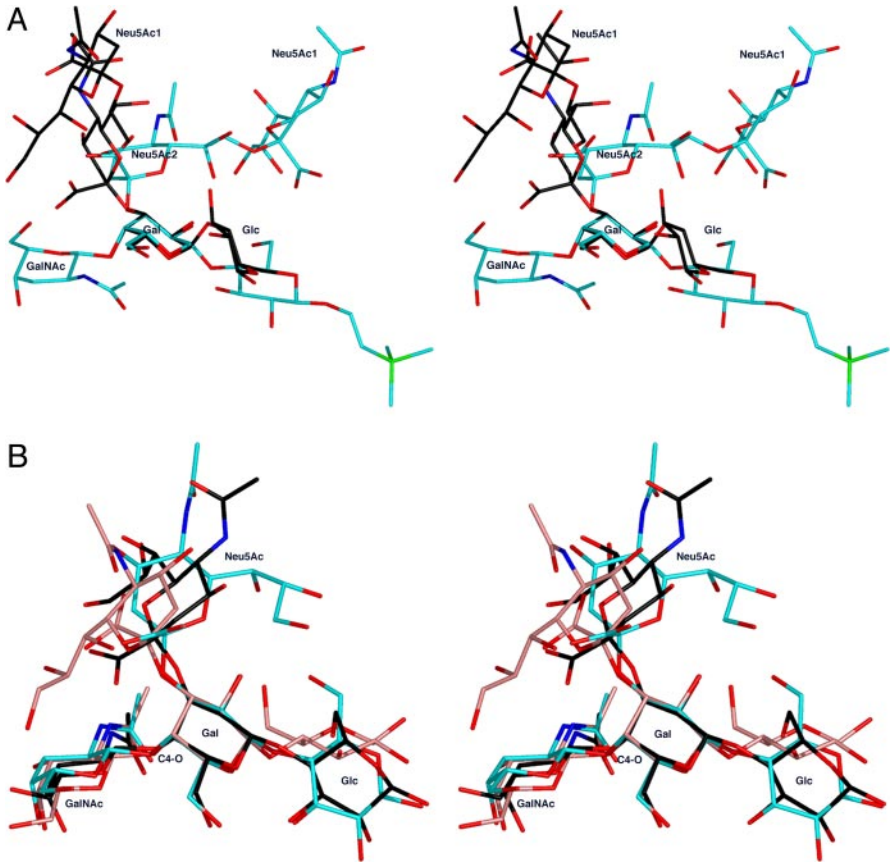

FIGURE 2. **Conformational comparison; GT1b with other glycans.** *A*, in this stereo image the GT1b analog (*cyan* carbon atoms) from the crystal structure of Siglec-7 has been superimposed over the Gal moiety with the GD3-like glycan (*black* carbon atoms) from a complex with tetanus toxin (PDB code 1YYN). Despite sharing the same core residues, the ligands differ significantly, and no two residues in sequence are superimposable. Torsion angles are given in Table 3. *B*, superimposition of the branch point at the Gal of GT1b (shown with *cyan* carbons), GM1 (PDB code 3CBH, *black*), and GT1bβ (PDB code 1FV2, *pink*) shows that the GalNAcβ(1,4)Gal linkage is highly restricted due to the presence of the branch and the axial position of the Gal C4-O (labeled C4-O). The Neu5Acα(2,3)Gal branch shows some restriction in conformational freedom but to a lesser extent. Note that the Neu5Ac of GT1bβ is in the non-natural β anomeric conformation.

TABLE 3

Glycosidic bond angles for disialyl ligands

The dihedral angles for the glycosidic bonds were analyzed using the CArbohydrate Ramachandran Plot (CARP) tool of the Carbohydrate Structure Suite (CSS) (44). For the linkage analysis for Neu5Ac-linked sugars torsion angles were determined in O (34). The dihedral angles for the β(1,4) linkages are defined as ϕ = O5-C1-O1-C′*X*, and ψ = C1-O1-C′*X*-C′*X* + 1. For the Neu5Acα(2,3)Gal linkage, ϕ = C1-C2-O3′-C3, and ψ = C2-O2-C3′-C4′. And for the Neu5Acα(2,8)Neu5Ac linkage, ϕ = C1-C2-O8′-C8′, ψ = C2-O8′-C8′-C7′, ω = C6′-C7′-C8′-C9′, and χ = C5′-C6′-C7′-C8′. The stereochemical conformation is given after the torsion angle and is defined as 0–30 synperiplanar (sp), 30° to 90° and −30° to −90° synclinal (sc), 90° to 150° and −90° to −150° anticlinal (ac), and −/+ 150° to 180° antiperiplanar (ap).

Sugar linkage	Dihedral angle (°); stereochemical arrangement			
	ϕ	ψ	ω	χ
GT1b-Siglec-7				
Galβ(1,4)Glcβ	−94.4; −sc	−131.7; −ac		
GalNAcβ(1,4)Galβ	−80.4; −sc	+136.2; +ac		
Neu5Acα(2,3)Galβ	−63; −sc	+124; +ac		
Neu5Acα(2,8)Neu5Acα	−152; ap/−ac	+77.8; +sc	+150; ap/+ac	+162; ap
dSL-tetanus toxin				
Galβ(1,4)Glcβ	−57.6 (+sc)	+150.7; +ac/ap		
Neu5Acα(2,3)Galβ	−84; −sc	+77; +sc		
Neu5Acα(2,8)Neu5Acα	−60; −sc	+127; +ac	+65; +sc	+163; ap

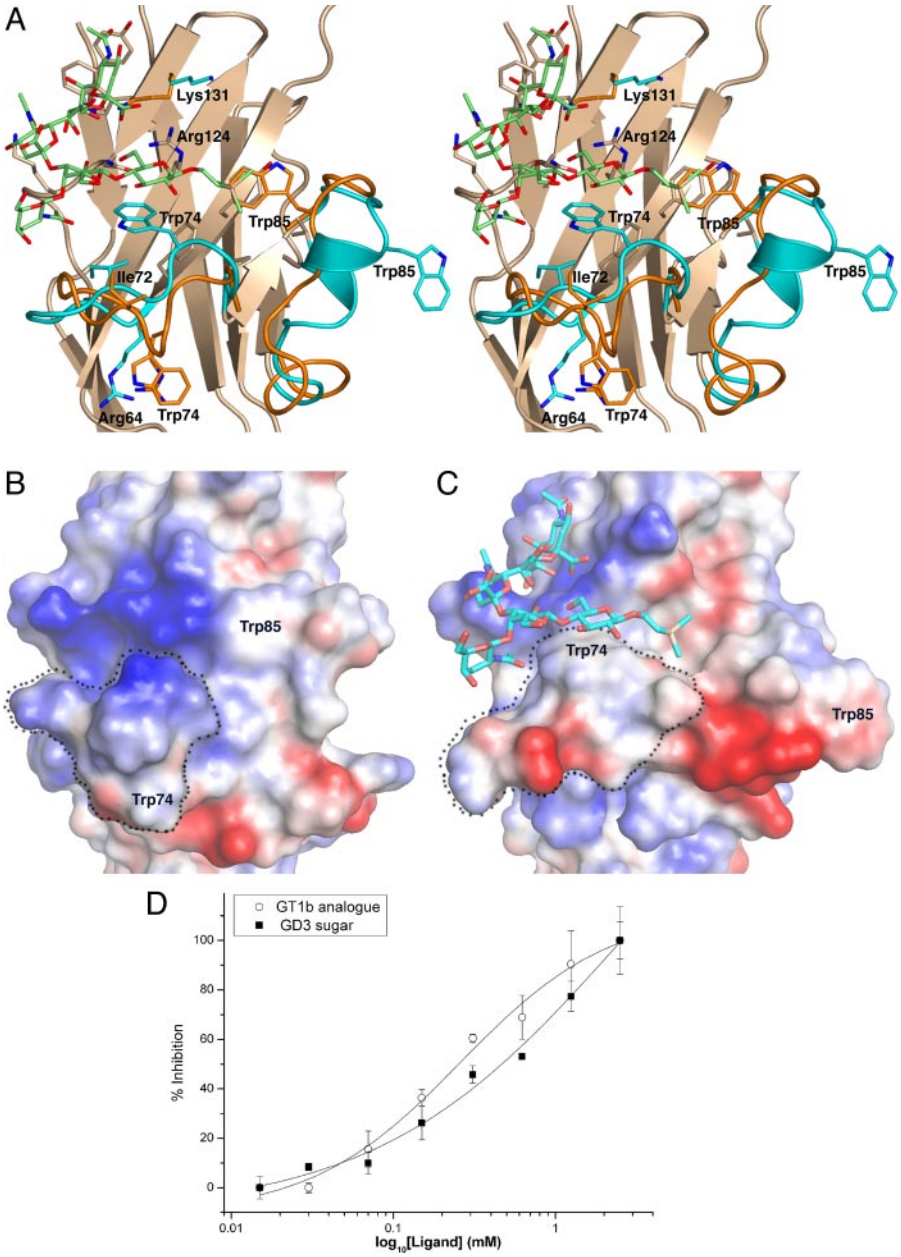

FIGURE 3. **Ligand-induced conformational changes.** Upon ligand binding two conformational changes occur. *A*, a stereo image shows a superimposition of the unliganded structure (PDB code 1OVS) and the GT1b complex. The regions in which a conformational shift is observed are shown with *orange* carbons for the apo form and *cyan* for the liganded. *Panels B* and *C* show the electrostatic surface potential of the apo and liganded forms, respectively (calculated using Adaptive Poisson-Boltzmann Solver countoured at −5 kT to +5 kT; basic regions are colored *blue*, and acidic regions are *red* (59). The C-C′ loop in the unliganded structure lies in an extended conformation, with a concave shape, giving the binding site a bowl-like character (*A* and highlighted with a *dotted line* in *B*). Upon the binding of GT1b, a major shift occurs in this loop, in particular, Trp-74, which lies under the loop, stacking against Arg-67 (*A* and *B*), is rotated so that it lies over the loop, becoming sandwiched between Ile-72 and the Glc of the ligand (*A* and *C*). In the liganded structure the C-C′ loop presents a hydrophobic convex shelf-like surface (highlighted by a *dotted line* in *C*) to the binding site over which the glycan branch point lies. In the C′-D loop region a further conformational change occurs. Trp-85, which lies across the surface, a point into a hydrophobic pocket (*A* and *B*), is displaced by the trimethylsilyl group, which buries itself in the pocket (*A* and *C*). Trp-85 flips out, becoming fully solvent exposed, causing the C′-D loop to adopt a helical conformation. As a result a large hydrophobic patch opens up on this side of the binding site (*C*). Whether this conformational change is artifactual, occurring because it is more energetically favorable to hide the trimethylsilyl group and expose the Trp to the solvent, or whether this may mimic some aspect of ganglioside binding (*i.e.* the ceramide head) is unclear. *D*, inhibition of binding of Siglec-7-Fc to GT1b by GT1b analog or GD3 oligosaccharide. Siglec-7-Fc was precomplexed with anti-Fc alkaline phosphatase and incubated with the indicated concentrations of each inhibitor before its addition to GT1b-coated microwells. The experiment was performed in triplicate at each dilution of inhibitor. The data were plotted using the Origin7.5 graph package, and IC_{50} values obtained using one site competition model in non-linear curve fitting. IC_{50} values were not found to be significantly divergent, indicating that the trimethylsilyl group is not a major determinant in the binding of the analog. 2.5 mM of lactose (data not shown) did not significantly hinder binding, showing that this interaction is sialic acid-dependent. Results shown are representative of three independent experiments.

presence or absence of a branch point. The branch point of GT1b, GalNAcβ(1,4)[Neu5Acα(2,3)]Galβ could conformationally restrict the molecule; overlaying the Gal of both ligands suggests that GalNAc would clash with the subterminal Neu5Ac were it in the equivalent position on the dSL glycan (Fig. 2*A*).

A further structural constraint imposed by the branch point in GT1b is rotation about the GalNAcβ(1,4)-Gal bond. A search of GalNAcβ-(1,4)Galβ torsion angles using the GlyTorsion tool at CSS (44) yielded 13 linkages (from 5 PDB entries, 3CHB, 2CHB, 1CT1, 1FV3, 1FV2, representing 2 unique proteins/ligands, cholera toxin/GM1 and tetanus toxin/GT1b-b analog (45–47)). All contain the branch-point GalNAcβ(1,4)[Neu5Acα(2,3)]Galβ and share ϕ angles in the -ac/-sc region (Table 3). All but one share ψ in the +ac region, supporting the notion that this branch point is conformationally restricted, as further evidenced by the striking superimposability of this branch point in the different glycans (Fig. 2*B*). This conformational restriction may, in part, result from the axial position of the Gal C4-O, which restricts the placement of the GalNAc.

Ligand-induced Conformational Changes—In most Siglec-7 crystal structures determined so far, the C-C′ loop is partially disordered (residues 69–72/73), suggesting that this loop is highly mobile (26, 27, 48). In the GT1b-Siglec-7 co-crystal structure the C-C′ loop is well ordered, with low B-factors, adopting a strikingly different conformation (Fig. 3). In all Siglec-7 crystal structures examined to date (Refs. 26, 27, and 48 and 10 crystal structures determined by the authors but unpublished), Trp-74 in the C-C′ loop is well ordered, lying under the C-C′ loop, packing against the hydrocarbon chain of Arg-64 (Fig. 3*A*). However, in the GT1b-Siglec-7 complex the side chain of Trp-74 lies above the C-C′ loop, having rotated ~260° (comparing the planes of the indole rings) and elevated by 6.9 Å (Cα to Cα),

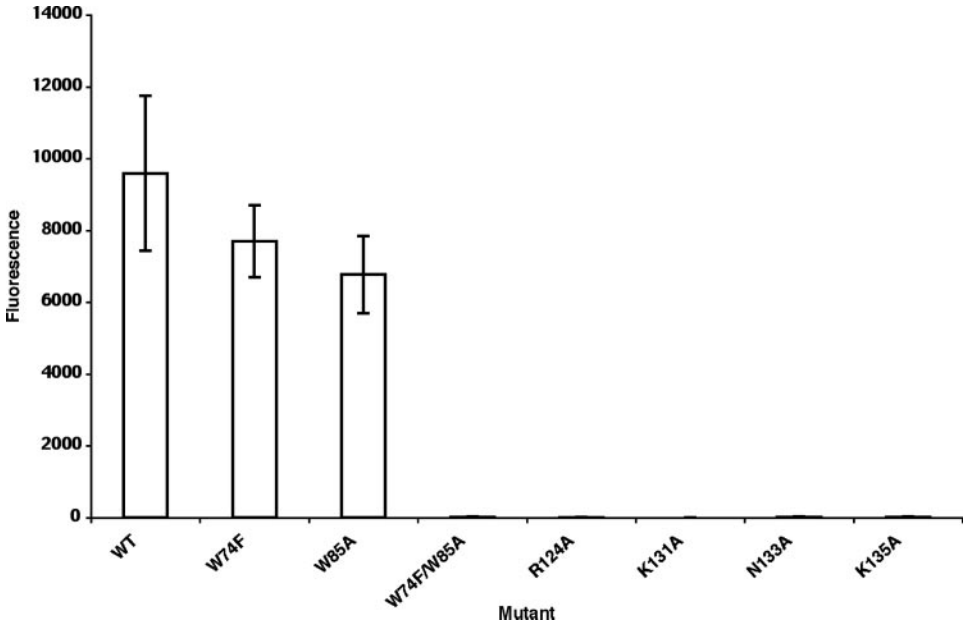

FIGURE 4. **GT1b binding by mutants of Siglec-7.** Site-directed mutagenesis was used to introduce mutations into pEE14-Siglec-7-Fc chimera construct. To test for GT1b binding the mutant Fc-chimeras were precomplexed with an alkaline phosphatase conjugated anti-Fc antibody and bound to GT1b ganglioside-coated microtiter plates. After the addition of the alkaline phosphatase substrate, fluorescein diphosphate, fluorescence measurements were taken. These results are representative of at least three independent experiments performed in triplicate. *WT*, wild type.

stacking with the Glc of GT1b. The position of Trp-74 is stabilized by Ile-72, which has rotated by ~100°, stacking below the indole ring. The conformation of the loop has changed significantly, with an average change in Cα position of 3.7 Å over 8 residues (Gly-69—Ala-76). As a consequence, the C-C′ loop loses its basic, bowl-like character and adopts a hydrophobic, slightly convex shelf, over which three sugars of GT1b lie (Fig. 3, *A* and *B*).

Additionally, another conformational change accompanies the binding of the GT1b analog; Trp-85, which lies in the center of the C′-D loop, is displaced, revealing a hydrophobic pocket (formed by Tyr-64, Phe-66, Pro-77, and Val-87) that interacts with the trimethylsilyl group (Fig. 3). As a result Trp-85 is flipped outward to a solvent-exposed position, and the C′-D loop adopts a helical conformation. Trp-85 moves by 6.1 Å (Cα to Cα), and the plane of the ring is rotated by ~200°. The overall shift of the backbone is very large, an average of 4.6 Å (Cα to Cα) over 11 residues (Pro-83 to Asp-93).

The trimethylsilyl group, which replaces the ceramide portion of the native ganglioside, appears to interact very favorably with Siglec-7. Naturally, the question arises of whether this group causes the ligand to interact in a non-physiological manner. However, it was not possible to directly compare this analog with the natural ganglioside in inhibition assays due to the formation of ganglioside micelles in the concentration range we wished to assay. Instead, we carried out inhibition assays comparing the GT1b analog with GD3 oligosaccharide (Fig. 3*C*). Previous studies (22) showed that Siglec-7 binds GT1b and GD3 with similar affinity, and therefore, the GD3 oligosaccharide is a suitable substitute for GT1b oligosaccharide, which was not available in the quantities required for inhibition assays. The IC_{50} values for both compounds were very similar, 0.26 (±0.02) mM for the GT1b analog and 0.39 (±0.6) mM for GD3 oligosaccharide. These results suggest that the sugar portion of the GT1b analog drives the binding and that the trimethylsilyl group does not contribute in a major way.

Site-directed Mutagenesis of Siglec-7—To evaluate the contribution that specific residues make to GT1b binding, we performed site-directed mutagenesis on a Siglec-7-Fc fusion construct. Several alanine substitution mutants were constructed of residues that directly contact the ligand or may indirectly be involved in the binding process. An alanine mutant of Trp-74 failed to express (presumably due to misfolding), so instead, the more conservative mutation to phenylalanine was made. A non-binding mutant was created by mutating the essential arginine to an alanine (R124A).

The mutants were screened for binding to GT1b ganglioside coated onto a 96-well plate (Fig. 4). As expected, mutation of Arg-124 abolished binding. Mutation of Asn-133 and Lys-135, which make multiple interactions with the ligand (Table 2), to alanine also lost the ability to bind GT1b. Mutation of Lys-131, which is predicted not to interact with the ligand, also abolished binding. This has been observed previously in red blood cell binding assays (27), where it was proposed that Lys-131 may protect the binding site from nonproductive, low affinity interactions (*e.g.* other sialylated ligands, solvent molecules, or anions) in its uncomplexed state.

Mutation of the C-C′ loop Trp-74, which stacks with the Glc moiety, to phenylalanine had little effect on ligand binding. Given the conservative nature of this mutation, the stacking interactions may be maintained. Similarly, mutation of Trp-85 to an alanine had little effect on binding, suggesting that this residue is not essential for the binding of GT1b. A double mutant, W74F/W85A, however, shows either no binding or severely reduced binding. This may be interpreted in two ways; that together these two residues contribute to the anchoring of the glycan reducing end/ceramide end of the molecule or that these mutations lead to a destabilization of the C-C′ loop, disrupting the binding of the sugar branch point.

DISCUSSION

The b-series gangliosides, which bear the disialyl motif, are candidate *in vivo* ligands for Siglec-7. Cytotoxicity assays have shown that an interaction between Siglec-7, expressed on NK cells, and GD3, expressed on target cells, can down-modulate NK killing (21). It is speculated that Siglec-7 may perform a protective role, recognizing such ligands as markers of "self" and preventing inappropriate NK activation. Such a role would support that of the inhibitory class of KIR molecules, which

recognize self major histocompatibility complex class I. The role of Siglec-7 could be especially important in the nervous system, where ganglioside expression is high (including the b-series gangliosides GD2 and GT1b), but major histocompatibility complex class I expression is low. Similarly, the expression of Siglec-7 ligands by major histocompatibility complex class I negative tumor cells could allow them to escape NK surveillance. Several cancer cell lines express elevated levels of b-series gangliosides *e.g.* GD2 and GD3 in melanoma, glioma, and neuroblastoma (49–51). Besides *trans* interactions with ligands on NK target cells, Siglec-7 is likely to interact *in cis* with ligands on NK cells, and such interactions could also be important for regulating NK cell activation. Recent observations suggest that NK cells express α(2,8)-disialylated ligands on their cell surface (52), adding further support to this possibility.

Such observations coupled with data from chimeric swap experiments prompted us to attempt to obtain a crystal complex of Siglec-7 in complex with a b-series ganglioside. Initial attempts to co-crystallize Siglec-7 with gangliosides failed. Using an analog of the GT1b ganglioside, in which a 2-(trimethylsilyl)ethyl group takes the place of the ceramide at the reducing end of the glycan, we were able to obtain a co-crystal, which diffracted to 1.85 Å. The replacement of ceramide with this smaller group may render it more amenable to crystallization (being more soluble, less flexible, and less likely to form micelles). The resulting Siglec-7 GT1b complex gives us a first glimpse at how siglecs may interact with gangliosides.

Examination of the complex revealed that five of the seven sugars were well ordered in the binding site and that a striking conformational change accompanied binding. The nonreducing end sialic acid is anchored by several hydrogen bonds with the protein backbone and side chains plus a stacking interaction with Trp-132. The α(2,8)-linked sialic acid makes very few hydrogen bonds, a water-mediated hydrogen bond with Asn-133 and a direct hydrogen bond with Lys-135. Both of these residues were shown to abolish binding when mutated to alanine. These residues make multiple contacts; Lys-135 interacts with both the sialic acids, and Asn-133 also interacts with the glucose at the reducing end. The branch point of the glycan lies over the C-C′ loop, a highly flexible loop, which changes conformation, enabling it to interact with the ligand. Another conformational change is observed in the C′-D loop due the displacement of Trp-85 by the highly hydrophobic trimethylsilyl moiety. Although the mutations W74F and W85A had little effect on GT1b binding, a double mutant showed reduced binding, indicating that this region may be important for anchoring the reducing end/ceramide head of the ganglioside.

These data can be interpreted within the framework of a previous study that used chimeric swaps between Siglec-7 and Siglec-9. Siglec-7 and -9 are highly related, sharing 80% sequence identity, but display distinct ligand binding preferences. Yamaji *et al.* (22) were able to show that replacing 6 residues from the tip of the C-C′ loop of Siglec-7 (Ala-70 to Lys-75) with those of Siglec-9 conferred Siglec-9-like binding characteristics. Swapping a region spanning the C-C′ loop, C′ strand, and the N-terminal half of the C′-D loop (Ala-68 to Gln-88 of Siglec-7) in Siglec-9 for those of Siglec-7 abolished all binding. However, replacement of an additional region in the G-G′ loop of Siglec-9 with residues 136–138 of Siglec-7 resulted in Siglec-7-like binding specificity. We interpret this region as being linkage-restrictive in Siglec-9, since in the co-crystal structure of Siglec-7-GT1b it does not make any contacts with the ligand, consistent with this being a non-restrictive feature. The G-G′ loop is highly variable among the siglecs (interestingly, in Siglec-8 there is a six-amino acid insertion in this loop; Fig. 1*E*). In Siglec-9 the sequence is HHR, whereas in Siglec-7 it is YDQ. This loop underlies the binding site and may influence its shape, and hence, the type of sialic acid linkages accessible to the siglec. Tyr-136 may influence it more directly as it stacks against the hydrocarbon chain of Lys-135.

The notion that the region Ala-68-Gln-88 of Siglec-7 is involved in directing ganglioside binding specificity is consistent with our observations. That the C-C′ of Siglec-9 is sufficient for conferring this specificity on Siglec-7 suggests that the rest of the Siglec-7 binding site can accommodate other linkages. The converse does not appear to be true, and replacement of additional residues in the G-G′ loop is required to confer binding on Siglec-9.

Glycans are highly flexible ligands, but a combination of molecular dynamics, molecular mechanics, NMR, and crystallographic studies have demonstrated that the conformation is often restricted to certain highly favored, low energy conformations and that lectins have evolved to bind certain conformers (42, 53). For a number of lectins there is a distinct conformer-dependent selection of ligands (54, 55). Such conformer selection may allow for additional hierarchies other than glycan composition in directing lectins to their physiological ligands, *i.e.* the permissive glycan conformation may only predominate when presented in a certain way and under particular physiological parameters.

By comparing the GT1b glycan structure with that of a GD3-like structure (dSL) we were able to observe large conformational differences throughout the molecule. The b-series gangliosides all share a common core of sugars, Neu5Acα(2,8)Neu5Acα(2,3)Galb(1,4)Glcβ, which is equivalent to GD3. The residues visible in the GT1b-Siglec-7 structure, GalNAcβ(1,4)[Neu5Acα(2,8)Neu5Acα(2,3)]Galβ(1,4)-Glcβ, are equivalent to GD2, but those that contribute the most to binding (the Neu5Acα(2,8)Neu5Acα head group and the reducing end Glc) are present within the GD3 substructure. From a simple model of the presence or absence of interacting sugars, we would expect Siglec-7 to have similar binding affinities for the b series gangliosides. This has been seen in some studies (22, 56); in others there is a clear rank order in binding affinity (22, 57). This variation may reflect differences in experimental conditions (in the way the gangliosides are presented, *e.g.* coated on microtiter plates or conjugated to streptavidin, buffering conditions, and ionic strength), which may also effect the conformation of the gangliosides and what proportion are in a conformation permissible for binding.

Understanding the differential ligand binding specificity displayed by members of Siglec family is key to defining the ligands they interact with *in vivo* and, hence, the functional importance of such interactions. This crystal structure shows that Siglec-7 specificity for b-series gangliosides is directed by multiple inter-

actions with the ganglioside sugars, which is accompanied by a conformational change in the C-C′ loop, which redefines the shape and character of the binding site. The high degree of sequence divergence in the C-C′ loop (and outlying regions) and the G-G′ loop may have a profound influence on the nature of the binding site, limiting or extending binding specificity. To truly define what directs ligand specificity, more extensive mutagenesis and binding studies must be performed, perhaps utilizing chimeric swap experiments with other CD33-related siglecs.

Acknowledgments—We are grateful for the time on beamline ID14-4 at the European Synchrotron Radiation Facility. The Consortium for Functional Glycomics, funded by NIGMS-GM62116, kindly provided the GD3 oligosaccharide used in inhibition assays.

REFERENCES

1. Crocker, P. R., and Varki, A. (2001) *Immunol.* **103,** 137–145
2. Angata, T., and Brinkman-Van der Linden, E. (2002) *Biochim. Biophys. Acta* **1572,** 294–316
3. Varki, A., and Angata, T. (2006) *Glycobiology* **16,** 1–27
4. Kannagi, R. (2002) *Curr. Opin. Struct. Biol.* **12,** 599–608
5. Crocker, P. R. (2002) *Curr. Opin. Struct. Biol.* **12,** 609–615
6. Kelm, S., Gerlach, J., Brossmer, R., Danzer, C. P., and Nitschke, L. (2002) *J. Exp. Med.* **195,** 1207–1213
7. Kelm, S., and Schauer, R. (1997) *Int. Rev. Cytol.* **175,** 137–240
8. Munday, J., Floyd, H., and Crocker, P. R. (1999) *J. Leukocyte Biol.* **66,** 705–711
9. Fruttiger, M., Montag, D., Schachner, M., and Martini, R. (1995) *Eur. J. Neurosci.* **7,** 511–515
10. Li, C., Tropak, M. B., Gerlai, R., Clapoff, S., Abramow-Newerly, W., Trapp, B., Peterson, A., and Roder, J. (1994) *Nature* **369,** 747–750
11. Patel, N., Brinkman-Van der Linden, E. C., Altmann, S. W., Gish, K., Balasubramanian, S., Timans, J. C., Peterson, D., Bell, M. P., Bazan, J. F., Varki, A., and Kastelein, R. A. (1999) *J. Biol. Chem.* **274,** 22729–22738
12. Crocker, P. R. (2005) *Curr. Opin. Pharmacol.* **5,** 431–437
13. Avril, T., Floyd, H., Lopez, F., Vivier, E., and Crocker, P. R. (2004) *J. Immunol.* **173,** 6841–6849
14. Nitschke, L., Carsetti, R., Ocker, B., Kohler, G., and Lamers, M. C. (1997) *Curr. Biol.* **7,** 133–143
15. Blixt, O., Collins, B. E., van den Nieuwenhof, I. M., Crocker, P. R., and Paulson, J. C. (2003) *J. Biol. Chem.* **278,** 31007–31019
16. de Graffenried, C. L., and Bertozzi, C. R. (2004) *Curr. Opin. Cell Biol.* **16,** 356–363
17. Falco, M., Biassoni, R., Bottino, C., Vitale, M., Sivori, S., Augugliaro, R., Moretta, L., and Moretta, A. (1999) *J. Exp. Med.* **190,** 793–802
18. Nicoll, G., Ni, J., Liu, D., Klenerman, P., Munday, J., Dubock, S., Mattei, M. G., and Crocker, P. R. (1999) *J. Biol. Chem.* **274,** 34089–34095
19. Angata, T., and Varki, A. (2000) *Glycobiology* **10,** 431–438
20. Ikehara, Y., Ikehara, S. K., and Paulson, J. C. (2004) *J. Biol. Chem.* **279,** 43117–43125
21. Nicoll, G., Avril, T., Lock, K., Furukawa, K., Bovin, N., and Crocker, P. R. (2003) *Eur. J. Immunol.* **33,** 1642–1648
22. Yamaji, T., Teranishi, T., Alphey, M. S., Crocker, P. R., and Hashimoto, Y. (2002) *J. Biol. Chem.* **277,** 6324–6332
23. Sato, C., Yasukawa, Z., Honda, N., Matsuda, T., and Kitajima, K. (2001) *J. Biol. Chem.* **276,** 28849–28856
24. Sato, C., Fukuoka, H., Ohta, K., Matsuda, T., Koshino, R., Kobayashi, K., Troy, F. A., and Kitajima, K. (2000) *J. Biol. Chem.* **275,** 15422–15431
25. Fox, D. A., He, X., Abe, A., Hollander, T., Li, L. L., Kan, L., Friedman, A. W., Shimizu, Y., Shayman, J. A., and Kozarsky, K. (2001) *Immunol. Investig.* **30,** 67–85
26. Alphey, M. S., Attrill, H., Crocker, P. R., and van Aalten, D. M. (2003) *J. Biol. Chem.* **278,** 3372–3377
27. Attrill, H., Takazawa, H., Witt, S., Kelm, S., Isecke, R., Brossmer, R., Ando, T., Ishida, H., Kiso, M., Crocker, P. R., and van Aalten, D. F. M. (2006) *Biochem. J.* **397,** 271–278
28. Ishida, H.-K., Ohta, Y., Tsukada, Y., Kiso, M., and Hasegawa, A. (1993) *Carbohydr. Res.* **246,** 75–88
29. Stanley, P., Caillibot, V., and Siminovitch, L. (1975) *Cell* **6,** 121–128
30. Otwinowski, Z., and Minor, W. (1997) *Methods Enzymol.* **276,** 307–326
31. Navaza, J. (2001) *Acta Crystallogr. D Biol. Crystallogr.* **57,** 1367–1372
32. Perrakis, A., Morris, R., and Lamzin, V. S. (1999) *Nat. Struct. Biol.* **6,** 458–463
33. Brunger, A. T., Adams, P. D., Clore, G. M., DeLano, W. L., Gros, P., Grosse-Kunstleve, R. W., Jiang, J. S., Kuszewski, J., Nilges, M., Pannu, N. S., Read, R. J., Rice, L. M., Simonson, T., and Warren, G. L. (1998) *Acta Crystallogr. D Biol. Crystallogr.* **54,** 905–921
34. Jones, T. A., Zou, J. Y., Cowan, S. W., and Kjeldgaard, M. (1991) *Acta Crystallogr. A* **47,** 110–119
35. Murshudov, G. N., Vagin, A. A., and Dodson, E. J. (1997) *Acta Crystallogr. D Biol. Crystallogr.* **53,** 240–255
36. Schuttelkopf, A. W., and van Aalten, D. M. (2004) *Acta Crystallogr. D Biol. Crystallogr.* **60,** 1355–1363
37. Suresh, M. X., and Veluraja, K. (2003) *J. Theor. Biol.* **222,** 389–402
38. Vasudevan, S. V., and Balaji, P. V. (2002) *J. Mol. Struct: THEOCHEM* **583,** 215–232
39. Crocker, P. R., Vinson, M., Kelm, S., and Drickamer, K. (1999) *Biochem. J.* **341,** 355–361
40. Feizi, T., and Mulloy, B. (2003) *Curr. Opin. Struct. Biol.* **13,** 602–604
41. Hirabayashi, J. (2004) *Glycoconj. J.* **21,** 35–40
42. Gabius, H. J., Siebert, H. C., Andre, S., Jimenez-Barbero, J., and Rudiger, H. (2004) *Chembiochem* **5,** 740–764
43. Vasudevan, S. V., and Balaji, P. V. (2002) *Biopolymers* **63,** 168–180
44. Lutteke, T., Frank, M., and von der Lieth, C. W. (2005) *Nucleic Acids Res.* **33,** 242–246
45. Fotinou, C., Emsley, P., Black, I., Ando, H., Ishida, H., Kiso, M., Sinha, K. A., Fairweather, N. F., and Isaacs, N. W. (2001) *J. Biol. Chem.* **276,** 32274–32281
46. Merritt, E. A., Kuhn, P., Sarfaty, S., Erbe, J. L., Holmes, R. K., and Hol, W. G. (1998) *J. Mol. Biol.* **282,** 1043–1059
47. Merritt, E. A., Sarfaty, S., Jobling, M. G., Chang, T., Holmes, R. K., Hirst, T. R., and Hol, W. G. (1997) *Protein Sci.* **6,** 1516–1528
48. Dimasi, N., Moretta, A., Moretta, L., Biassoni, R., and Mariuzza, R. A. (2004) *Acta Crystallogr. D Biol. Crystallogr.* **60,** 401–403
49. Pukel, C. S., Lloyd, K. O., Travassos, L. R., Dippold, W. G., Oettgen, H. F., and Old, L. J. (1982) *J. Exp. Med.* **155,** 1133–1147
50. Urmacher, C., Cordon-Cardo, C., and Houghton, A. N. (1989) *Am. J. Dermatopathol.* **11,** 577–581
51. Wikstrand, C. J., Fredman, P., Svennerholm, L., and Bigner, D. D. (1994) *Prog. Brain Res.* **101,** 213–223
52. Avril, T., North, S. J., Hasam, S. M., Willison, H. J., and Crocker, P. R. (2006) *J. Leukocyte Biol.*, in press
53. Roseman, S. (2001) *J. Biol. Chem.* **276,** 41527–41542
54. Gilleron, M., Siebert, H. C., Kaltner, H., von der Lieth, C. W., Kozar, T., Halkes, K. M., Korchagina, E. Y., Bovin, N. V., Gabius, H. J., and Vliegenthart, J. F. (1998) *Eur. J. Biochem.* **252,** 416–427
55. Siebert, H. C., Andre, S., Lu, S. Y., Frank, M., Kaltner, H., van Kuik, J. A., Korchagina, E. Y., Bovin, N., Tajkhorshid, E., Kaptein, R., Vliegenthart, J. F., von der Lieth, C. W., Jimenez-Barbero, J., Kopitz, J., and Gabius, H. J. (2003) *Biochemistry* **42,** 14762–14773
56. Ito, A., Handa, K., Withers, D. A., Satoh, M., and Hakomori, S. (2001) *FEBS Lett.* **504,** 82–86
57. Rapoport, E., Mikhalyov, I., Zhang, J., Crocker, P., and Bovin, N. (2003) *Bioorg. Med. Chem. Lett.* **13,** 675–678
58. Higgins, D. G., Thompson, J. D., and Gibson, T. J. (1996) *Methods Enzymol.* **266,** 383–402
59. Baker, N. A., Sept, D., Joseph, S., Holst, M. J., and McCammon, J. A. (2001) *Proc. Natl. Acad. Sci. U. S. A.* **98,** 10037–10041
60. Vriend, G. (1990) *J. Mol. Graph.* **8,** 52–56